Available online at www.sciencedirect.com
SCIENCE DIRECT®
ELSEVIER
Applied Surface Science 210 (2003) 54–60
applied surface science
www.elsevier.com/locate/apsusc

Tribology and ultrasonic hysteresis at local scales

R. Szoszkiewicz[a,*], B.D. Huey[a], O.V. Kolosov[b], G.A.D. Briggs[b], G. Gremaud[a], A.J. Kulik[a]

[a]*Ecole Polytechnique Federale de Lausanne, FSB-IPMC, Nanomechanics Group, CH-1015 Lausanne, Switzerland*
[b]*Department of Materials, Oxford University, OX1 3PH, UK*

Abstract

Local adhesion hysteresis (AH) is difficult to measure using an AFM due to complications introduced by compliant cantilevers as they snap-in and snap-out to/from a sample surface. But, at ultrasonic frequencies well above the cantilever mechanical resonance, the effective stiffness can increase enormously. Therefore, ultrasonically vibrating a sample in contact with an AFM tip can probe the hysteretic cycle of tip–sample in- and out-interactions [Jpn. J. Appl. Phys. 32 (1993) 22; Acoust. Imag. (1996)] allowing AH to be investigated by measuring ultrasonic hysteresis (UH). For the first time UH is compared here with lateral force microscopy (LFM) data. The same kind of experiments is also implemented for a nanoindenter based setup. Thus, the *micro-* (nanoindenter) and *nano-* (AFM) scales are investigated. UH and friction of both length scales are found to be linearly related for surfaces differing widely in elasticity and adhesion.

PACS: 46.30.Pa; 61.16.Ch; 06.30.Bp; 43.35Zc

Keywords: Ultrasonic force microscopy; Adhesion hysteresis; Friction; Nanoindentation; Heterodyne interferometry

1. Introduction

For an insight into adhesive material properties, an AFM is usually applied with force modulation. There are, however, certain constraints due to cantilevers. Compliant levers are subjected to a large mechanical hysteresis [3], while the use of stiff cantilevers, with a few exceptions [4], decreases the sensitivity and overall contrast. To overcome these difficulties a family of techniques applying ultrasonic excitations was developed [2]. In this paper, ultrasonic force microscopy (UFM) is exploited to investigate relations between adhesion hysteresis (AH) and friction.

UFM takes advantage of inertial stiffness which adds to the elastic stiffness of the cantilever due to high frequency vibrations. When ultrasonic excitation with a given amplitude a is applied to the sample, the cantilever experiences an average force $\bar{F}(\delta)$ known as the ultrasonic force [1]. Such a mean force is determined by averaging over the force–distance curve between tip and sample for the entire vibration amplitude, where δ is an indentation and/or separation with δ_0 as the initial indentation value. Modulating the vibrations by a frequency at which the cantilever can readily respond (Fig. 1(a)) causes the lever to deflect from its initial position z_0 by an extra term $\bar{z}_t$ arising from the difference between initial and averaged tip–sample forces as

* Corresponding author. Tel.: +41-21-693-4474; fax: +41-21-693-4470.
E-mail address: robert.szoszkiewicz@epfl.ch (R. Szoszkiewicz).
URL: http://www.ipmc.epfl.ch

0169-4332/03/$ – see front matter
doi:10.1016/S0169-4332(02)01479-4

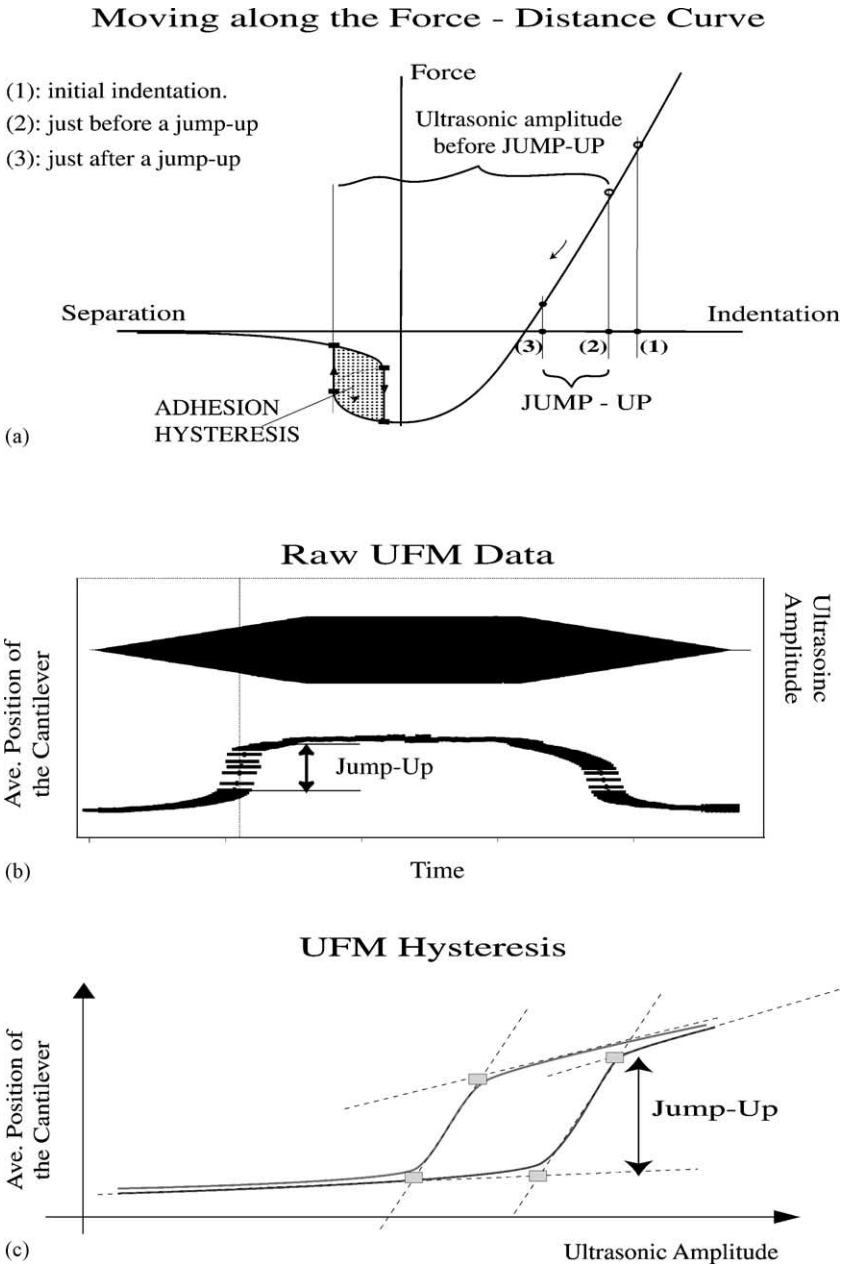

Fig. 1. (a) *F–d* curve based on JKRS contact mechanics [18]. (1) Marks initial tip position without ultrasounds. The mean indentation changes from (1) to (2) when the ultrasounds amplitude is increased. Once contact is lost during a cycle of vibrations the mean force changes abruptly in order to maintain the equilibrium (Eq. (1)) and a new mean indentation at point (3) is established. (b) Raw UFM data. (c) Resulting UFM Hysteresis.

imposed in Eq. (1) [1]:

$$k_c(\bar{z}_t + z_0) = \bar{F}(\delta) = \left(\frac{1}{2a}\right)\int_{\delta_0-\bar{z}_t-a}^{\delta_0-\bar{z}_t+a} F(\delta) \qquad (1)$$

$\bar{z}_t$ is very small for small ultrasonic amplitudes, since the nonlinearities of the *F–d* curve are negligible and the mean value $\bar{F}(\delta)$ stays around $\bar{F}(\delta_0)$. For higher amplitudes the average force may change suddenly if

an abrupt loss of contact occurs during the ultrasonic period. Thus, for a trapezoidal modulation of the ultrasonic amplitude and only slow feedback on, the averaged cantilever position may *jump-up* (Fig. 1(b)) on increasing the vibrational amplitude, and *jump-down* on decreasing the modulation amplitude. Both jumps occur at different ultrasonic amplitudes, since the mean tip indentations before jump-up and jump-down are necessarily different. The resulting UFM data (Fig. 1(c)) exhibits a hysteretic behavior and the area between the two curves is defined as the UFM Hysteresis Area.

UFM Hysteresis depends mostly on elastic and adhesive contributions of the tip–sample contact [5] and is believed to scale with AH. AH is defined as the difference of the work necessary for separating two surfaces and gained on bringing them together, and is closely related to friction [9,10]. Such correlations have been demonstrated, i.e. in studies of the adhesion and friction of adsorbed surfactant layers with each other [6] and of polymer surfaces with mica [7,8]. Apart from elastic and adhesive sources, AH can be due to chemical effects. Here, we do not necessarily mean chemical reactions, but rather relaxation or reconfiguration of surface molecules during contact [11–13]. In addition, AH should be distinguished from the mechanical tip hysteresis giving rise to snap-in and snap-out behavior [14]. Also the presence of capillary forces under ambient conditions should be rather associated with a ''capillary force hysteresis'' [3]. It is important to investigate the correlation between AH and friction, since it could lead to localized, calibrated friction measurements.

2. Experimental

The experimental setup (Fig. 2(a)) for the nanoscale measurements is based on a PSI CP AFM. A piezoelectric transducer is fixed underneath the sample. The silicon AFM cantilever tip is initially in contact with the specimen with nN setpoint forces applied. To reduce the impact of capillary forces the experiments are performed in a dry glove box with controlled relative humidity of $5 \pm 1\%$. The details of UFM are as follows. The modulated frequency (HF) is usually of the order of MHz, set to be near a piezotransducer thickness mode. The modulating frequency (LF) is usually of the order of 100 Hz. Microscope feedback is kept as low as possible in order to maintain the contact setpoint force while not influencing the cantilever response. A heterodyne interferometer with a working bandwidth (20 kHz–60 MHz) [15] is used in situ to detect any lever motion at high frequencies with picometer accuracy. The LF lever deflection is detected using the standard laser beam deflection. This yields a signal of the order of a few mV from the photodetector, which is calibrated to distance units by passing the same tip across steps of known height (22 nm height steps, MT-NDT standard).

After UFM measurements on each sample, friction data are immediately collected using the lateral force microscopy (LFM) signal from a friction loop [16], which measures lateral cantilever bending during a scan and is generally not calibrated. To obtain the relation between lateral and normal forces, the LFM data are collected for varying setpoint values and LFM vs. setpoint curve is then fit [17]. Thus, friction at high loads can be obtained. Here, high loads mean friction at high setpoint values of about 100 nN. Scans of $3\,\mu m \times 3\,\mu m$ are taken to avoid common artifacts due to nano-scale sample heterogeneities and scanner acceleration at scan extremities. The scan speed is 1 Hz so that relative effects of stick-slip are marginal and a scan speed dependence [10] is avoided.

The nanoindenter experiment (Fig. 2(b)) is based on a *X*, *Z* Picoindenter from Hysitron Inc. mounted on a PSI CP AFM. Berkovitch diamond tips are used in these studies. Unlike the AFM, this instrument can sense vertical as well as lateral *calibrated* displacements and forces. The choice of UFM frequencies is also substantially different for the nanoindenter than for the AFM. As the load cell is inherently stiffer, a modulated frequency of a few kHz is applied. It is still higher than the tip contact resonance and ensures well its dynamic stiffness. LF is two orders of magnitude lower than HF. Typical setpoints are of the order of a few μN.

After completing UFM measurements with the nanoindenter, the friction is determined by performing scratch tests over 5 μm distances with small load forces (about 20 μN) to avoid destroying the surface. From such tests a friction coefficient is obtained by dividing the measured lateral by applied normal force. Nanoindenter measurements are performed in laboratory atmosphere (about 30% of relative humidity),

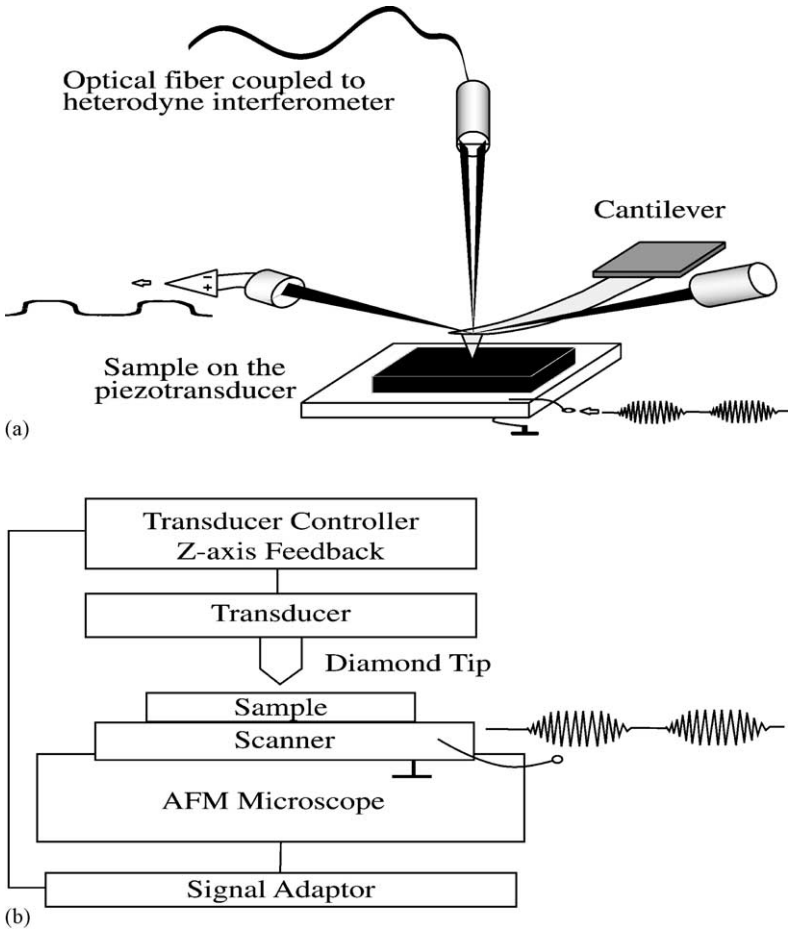

Fig. 2. (a) AFM setup. The AFM tip is in contact with a sample fixed to a transducer for ultrasonic excitations. Cantilever position is detected by laser beam deflection and a heterodyne interferometer. (b) Nanoindenter setup. An indenter tip is in contact with sample and AFM scanner is modulated directly.

since capillary forces did not produce any detectable change in resulting UFM spectra.

In both cases (AFM + nanoindenter), UFM and friction measurements were performed on a series of metallic samples of high purity (99.99%): Pt, Au, Cu, Zn, Ti, Fe and Nb from Goodfellow, as well as muscovite mica and calcite from Baltex. Metallic samples were prepared via mechanical polishing and then cleaned in an ultrasonic bath before measurements. Mica and calcite were cleaved at room conditions just before measuring. The r.m.s. roughness of all samples was generally of the order of angstroms over 3 μm × 3 μm AFM images.

AFM based measurements were also conducted with a series of perfluorinated silanes deposited on the glass substrate via gas phase silanization [19]. They form stable and homogeneous monolayers with pretty much the same elastic properties (Young's moduli), but adhesion energy increasing with monolayer density.

3. Results and discussion

The UFM Hysteresis correlates very well with friction for the nanoindenter measurements (Fig. 3(a)).

These results should be insensitive to nanometer scale inhomogeneities as measurements employ μN loads, contact radii of the order of 100 nm and indentation depths of a few nm. To determine nm scale properties, the sharper contact radius provided by an AFM should be applied. But before considering the same set of samples as those studied with the nanoindenter. Fig. 3(b) presents UFM results

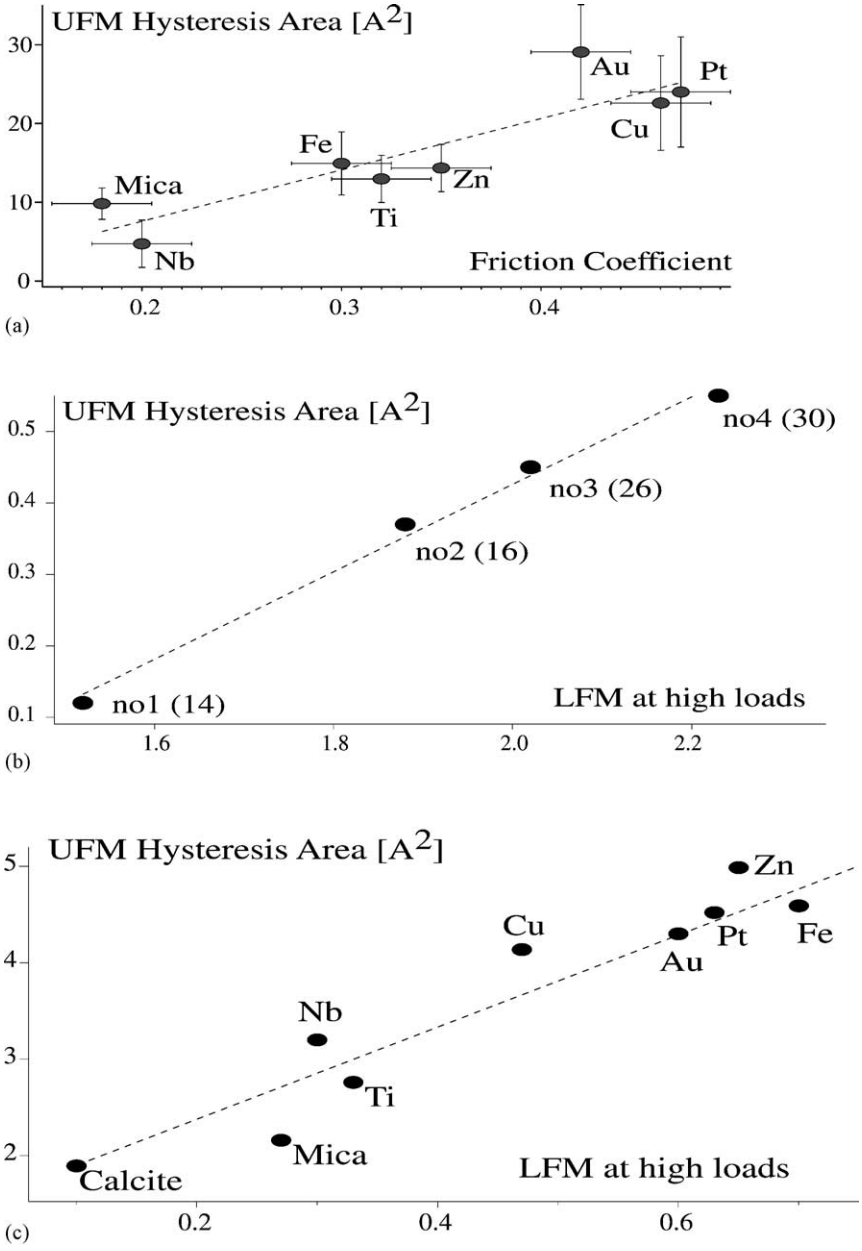

Fig. 3. (a) UFM Hysteresis Area vs. friction measured by the nanoindenter. Error bars show relative errors also for next plots, since they come from averaging several data waveforms measured at one spot. (b) UFM Hysteresis Area vs. friction at high loads measured with an AFM for a fluorosilanes monolayers of varying adhesion energy in mJ/m^2 as indicated in brackets. (c) Samples like in Fig. 3(a), but measured with an AFM.

for a series of silanes. Again, there is a strong correlation between ultrasonic hysteresis (UH) and friction and UFM Hysteresis Area increases with adhesion energy, as predicted in simulations [20], due to which the correlation between UH and friction should be dominated by adhesion and offset by elastic differences. Reliability of these nano-scale measurements encouraged the metalic + mica and calcite samples investigations by AFM. Fig. 3(c) plots the resulting UFM Hysteresis Area compared to LFM at high loads. Calibration of the LFM signal is possible [16], but has not been performed, so absolute comparisons must wait for future work.

The important difference between nano- and micro-scale measurements manifests itself in the magnitude of the UFM response-approximately one order of magnitude greater for the nanoindenter than for the AFM. This is thought to be related to the relative differences in the contact areas for these two measurements. The contact area for the nanoindenter experiments may be found as follows: from the indentation curves (knowing the setforce value) one reads the corresponding contact depth. Contact depth is then related directly to the contact area (S_{NI}) via an indenter calibration curve produced for each tip at the beginning of experiments. Thus, S_{NI} was found to be about 2000 nm^2 for used samples and setpoint forces. When working with the AFM, the lower limit for the contact radii contact radius a can be estimated by DMT mechanics [18]. Let R be the reduced contact curvature. It has been estimated to be about 20–50 nm (changes during the experiment) by scanning the tip across a grating of sharped needles (NT-MDT calibration grating). Then: $a = (R(F + 2\pi Rw)/K)^{1/3}$, where K is the reduced Young's modulus, w the adhesion energy, F the AFM setpoint force. The corresponding contact areas $S_{AFM} = \pi a^2$ are found to be about 80–300 nm^2. The comparison of contact surfaces for AFM (S_{AFM}) and nanoindenter (S_{NI}) gives a ratio of (S_{NI}/S_{AFM}) ranging from 7 to 25, so as the UFM Hysteresis Areas normalized via dividing by the corresponding contact areas become comparable. Such a normalization comes because the contact forces, F, are proportional to $(1/R)$, indentation δ scales with $(1/R)^{1/3}$ and the contact radius a with $(1/R)^{2/3}$. Thus, $\Delta F \times \Delta\delta$, the AH to which UFM Hysteresis is proportional, will scale with a^2.

A careful inspection of plots from Fig. 3(a) and (c) reveals that the relative position of several samples has shifted, e.g. Fe, Cu, Nb. This may result from the enhanced AFM sensitivity over the nanoindenter to surface defects, random dust particles, water aggregates or surface contaminations depositing from the air. Increasing statistics, i.e. making measurements at more than 1 sample point, should however mask the effect of surface inhomogeneities and preserve the proportionality between UFM and friction unless the surface structure transform during the time between UFM and friction measurements. Also the presence of oxides, sulfates and other topographical features contributes to the measurements, since even a thin oxide layer may significantly alter the adhesion and consequently AH. Any eventual diffusion and important surface reorganization during UFM measurements are minimal due to high frequency of the tip–surface interaction. Thus, UFM has a great potential for investigating fast adhesion events.

Finally, the correlation between UFM Hysteresis Area and friction over different length scales and loading conditions is not unexpected. The lateral cantilever stiffness is usually about two orders of magnitude higher than the normal stiffness, making it comparable to the dynamic stiffness of the tip in UFM experiments. Therefore UFM Hysteresis is scaling with AH and consequently with friction.

4. Conclusions

UFM has been shown to be a useful tool for determining local friction by simply measuring the UH. The technique is applicable at both micro- and nano-scales and seems to scale with the contact area. Finally, the correlation between UFM Hysteresis and local friction has been demonstrated for silanes films with fixed elastic properties and varying adhesion energy, as well as for broad range of engineering materials.

Acknowledgements

The authors acknowledge Dr. Gerit Jaenchen for providing silane samples and their adhesion energies measurements.

References

[1] O. Kolosov, K. Yamanaka, Jpn. J. Appl. Phys. 32 (1993) 22.
[2] O. Kolosov, G.A.D. Briggs, K. Yamanaka, W. Arnold, Nanoscale imaging of mechanical properties by UFM, Acoust. Imag. 22 (1996).
[3] N.A. Burnham, A.J. Kulik, Surface forces and adhesion, in: Handbook of Micro/Nanotribology, CRC Press, Boca Raton, 1999.
[4] P. Hoffmann, A. Oral, R.A. Grimble, H.O. Ozer, S. Jeffery, J.B. Pethica, Proc. Roy. Soc. Lond. A 457 (2001) 1161.
[5] F. Dinelli, M.R. Castell, D.A. Ritchie, N.J. Mason, G.A.D. Briggs, O.V. Kolosov, Philos. Mag. A 80 (2000) 2299.
[6] Y.-L. Chen, C.A. Helm, J.N. Isrelachvili, J. Phys. Chem. 95 (1991) 10736.
[7] M. Heuberger, G. Luengo, J.N. Israelachvili, J. Phys. Chem. B 103 (1999) 10127.
[8] G. Luengo, M. Heuberger, J.N. Israelachvili, J. Phys. Chem. B 104 (2000) 7944.
[9] J.N. Israelachvili, Intermolecular and Surface Forces, 2nd ed., Academic Press, London, 1998.
[10] B.N.J. Persson, Sliding Friction: Physical Principles and Applications, Springer, Berlin, 1998.
[11] M. Tirrell, Langmuir 12 (1996) 4548.
[12] M.K. Chaudhury, M.J. Owen, J. Phys. Chem. 97 (1993) 5722.
[13] F.-J. Scmitt, H. Yoshizawa, A. Schmidt, G. Duda, W. Knoll, G. Wegner, J.N. Israelachvili, Macromolecules 28 (1995) 3401.
[14] B. Cappella, G. Dietler, Surf. Sci. Rep. 34 (1999) 1.
[15] P. Vairac, B. Cretin, Opt. Commun. 132 (1996) 19.
[16] D. Gourdon et al., Tribol. Lett. 3 (1997) 317.
[17] U.D. Schwarz, O. Zwoerner, P. Koester, R. Wiesendanger, Phys. Rev. B 56 (1997) 6987.
[18] D. Maugis, Contact, Adhesion and Rupture of Elastic Solids, Springer, Berlin, 2000.
[19] G. Jaenchen, Patent Pending.
[20] B.D. Huey, G.A.D. Briggs, O.V. Kolosov, J. Appl. Phys., submitted for publication.